Supporting information

MOF-Derived CuO/TiO_2 Photocatalyst for Methanol Production from CO_2 Reduction in an AI-Assisted Continuous Flow Reactor

Bhavya Jaksani[ab], Ruchi Chauhan[bc], Switi Dattatraya Kshirsagar[a], Abhilash Rana[bc], Ujjwal Pal [* ab] and Ajay K. Singh [* bc]

a. Department of Energy & Environmental Engineering, CSIR-Indian Institute of Chemical Technology, Tarnaka, Hyderabad, Telangana-500007, India, E-mail: upal03@gmail.com.

b. Academy of Scientific & Innovative Research (AcSIR), Ghaziabad, Uttar Pradesh-201002, India.

c. Department of Organic Synthesis and Process Chemistry, CSIR-Indian Institute of Chemical Technology, Hyderabad 500007, India, E-mail: ajaysingh015@iict.res.in; ajaysingh015@gmail.com.

Contents

Experimental section

1.1 Materials

Copper nitrate trihydrate (Sigma Aldrich, Cu $(NO_3)_2.3H_2O$), trimesic acid (Sigma Aldrich, H_3BTC), N, N dimethyl formamide (Sigma Aldrich, DMF), ethanol (Sigma Aldrich, C_2H_6O), titanium isopropoxide (Avra, (Ti $\{OCH(CH_3)_2\}_4$), D.I H_2O. PFA (id = 4 mm) tubing, T-junction, high-purity PFA tubing was purchased from Upchurch IDEX HEALTH &SCIENCE. The photo-batch reactor bought from Lelesil Mumbai India was slightly modified for the continuous flow reaction. White LFD light reactor was bought from the Smartchemsynth Machine Pvt. Ltd, Hyderabad.

1.2 Synthesis of CuMOF (CuBTC)

CuMOF is synthesized according to previously reported literature with slight modifications.[1] In a typical procedure, add 1.039 grams of copper nitrate (Cu $(NO_3)_2.3H_2O$) in 7.5 mL of deionized water. Stir the mixture vigorously at room temperature for 30 minutes until Cu $(NO_3)_2.3H_2O$ is completely dissolved. Next, in another round bottomed flask, take 7.5 mL of each of DMF, C_2H_6O, and 0.903 grams of H_3BTC and stir for 30 minutes until they are fully dissolved. Then combine both the solutions and stirring is continued. Later, transfer the mixed solution to a 100 mL Teflon-lined stainless-steel autoclave and hydrothermally treated at 120 °C for 12h. Afterward, the autoclave was allowed to cool down to room temperature, and a blue coloured precipitate was formed by centrifugation. The resultant precipitate washed with DMF followed by methanol for three times, then dried at 80 °C to obtain a Cu-MOF nanocomposite sample.

1.3 Synthesis of MCT-100 (MOF derived CuO/TiO_2)

The final photocatalyst (MCT-100) is prepared by taking 20 mL of 4:1 ethanol/water mixture in to a round bottomed flask and 100 mg of Cu-BTC, sonication is done for 30 minutes to fully disperse the particles. Then add dropwise 2.5 mL of titanium isopropoxide (Ti$\{OCH(CH_3)_2\}_4$) with continuous stirring and maintain stirring for 12h in an inert atmosphere. The precipitate is obtained by centrifugation, wash it with ethanol for three times followed by water, dried it in oven for whole night. The obtained precipitate is calcined at 450 °C for five hours in N_2 atmosphere at ramping rate of 5°C/min. The same procedure is

done with the different amounts of CuBTC (10 mg, 50 mg and 200 mg) by taking the constant amount of titanium isopropoxide to obtain MCT-10, MCT-50, and MCT-200 respectively. [2]

1.4 Synthesis of TiO_2

The TiO_2 is prepared by taking 20 mL of 4:1 ethanol/water mixture in to a round bottomed flask. Then dropwise add the 2.5 mL of titanium isopropoxide ($Ti\{OCH(CH_3)_2\}_4$) with continuous stirring for 12h in an inert atmosphere. The precipitate is obtained by centrifugation, wash it with ethanol for three times followed by water, dried it in oven for whole night. The obtained precipitate is calcined at 450 °C for five hours in N_2 atmosphere at ramping rate of 5°C/min

1.5 Characterization

The structural phase analysis of the as-synthesized photocatalysts was performed by using Powder X-ray diffraction patterns (XRD) on a Bruker AXS diffractometer (D8 advance) at a generator voltage of 40 kV and current of 30 mA using Cu-Kα1 irradiation (λ = 1.5406 Å). The sample was scanned in the 2θ = 10-80° range with a scan rate of 1 s/step. X-ray photoelectron spectroscopy (XPS) was performed via a Kratos (axis 165) analytical instrument with Mg Kα irradiation. About 10-9 Torr pressure was maintained in the spectrometer. The structural morphology of the photocatalysts was examined by using MIRA3 FEG-SEM (TESCAN) Scanning electron microscopy (SEM) at an accelerating voltage of 5 kV. Transmission electron microscopy (TEM) image of the representative photocatalysts was obtained by using a JEOL 2010EX TEM instrument equipped with the high-resolution style objective-lens pole piece at an acceleration voltage of 200 kV fitted with a CCD camera. N_2 adsorption-desorption isotherms of the photocatalysts were obtained on a Quanta chrome Nova 2200e gas adsorption analyzer at 77 K. The optical properties were characterized by using UV-Vis diffuse reflectance spectroscopy (DRS) Perkin Elmer Lambda 750 instrument using $BaSO_4$ as a reference. The sample has been placed in the sample holder for the measurement and the light is allowed to pass through the sample which leads to the absorption of the light and the light transmitted by the sample has been recorded. The Photoluminescence (PL) spectra were recorded using a Fluorolog-3 spectrofluorometer (Spex model, JobinYvon) at their respective excitation (λex) wavelength. Fluorescence Lifetime decay measurements were carried out by using time-correlated singlephoton counting

(TCSPC) setup (Fluorolog-3 Triple Illuminator, IBH Horiba Jobin Yvon). Briefly, the samples were excited at 380 nm, and the emission was observed at 480 nm.

1.6 Photo-electrochemical studies:

The entire photo-electrochemical test was carried out in the electrochemical workstation. 0.25 M aqueous solution of Na_2SO_4 was used as an electrolyte for all experiments. Pt wire and calomel electrodes were used as counter and reference electrodes. The preparation of the working electrode is carried out using 20 µL of suspension (5 mg in 1mL ethanol) on ITO coated glass surface with a specific area of 2 cm^2. The light source is considered as an Photoelectrochemical measurements at room temperature were recorded on the CH Instruments Inc., USA, CHI6005E, Electrochemical Workstation with Potentiostat using a three-electrode system with a standard three-electrode system with the photocatalyst-coated ITO as the working electrode, Pt wire as the counter electrode, SCE electrode as the reference electrode. The artificial solar simulator of AM 1G illuminator (100 mW cm^{-2}) was used as the light source during the measurement. The electrochemical cell was a conventional 7 three-electrode cell with a 3 mm thick Pyrex glass.

1.7 Photocatalytic methanol production through batch mode

The photocatalytic conversion of carbon dioxide to methanol is tested for all as synthesised catalysts. The photocatalytic reaction was carried out in 25 ml quartz reactor with reaction solution of 7 ml DMF + 1ml H_2O with 50 mg of photocatalyst sealed with airtight rubber septum and degassed and purging with nitrogen for 15 min to remove dissolved gases and was purged with CO_2 for 30 min for saturating the solution with CO_2. Then the reaction mixture was irradiated with carbon dioxide balloon for 4 hours using 420 W Xe lamp. The quantitative determination (conversion) of the reactions were analyzed by gas chromatography (GC) employing chromatograph (Perkin Elmer Clarus 590) equipped with flame ionization detector (FID). Columns (Stabilwax w/Integra-Guard column) were employed for the quantification of the products. flow rate: 0.5 mL min-1, injector temperature:250°C, FID detector temperature: 260°C) for determination of liquid products. A calibration curve of the CO_2 gas is set to in determining the linear response over the GC-FID system. Few neat reactions were carried out to establish that MeOH synthesis was caused by the photoreduction of CO_2. Under similar experimental circumstances, a blank reaction was performed through the light irradiation without any suspension of the photocatalyst in the solution, and the other reaction doesn't include any light irradiation while the highest efficiency would be obtained on light irradiation,

with continuous carbondioxide flow. Here we have calculated the apparent quantum efficiency of CuO/TiO_2 towards the photocatalytic reduction of CO_2 towards methanol generation, at 420 ± 20 nm. The catalytic reaction mixture was irradiated under a 400 W LED lamp.

$$N_{photon} = \frac{P\lambda t}{hc}$$

Here, P = Power in terms of intensity of the light that is incident over the catalyst surface, (0.19 J s^{-1} cm^{-2}), specific surface area =6 cm^2, λ = wavelength (400 nm), t = time spent over the reaction for light irradiation (4 h), h = Planck's constant (6.626 x 10^{-34} J s), whereas h= velocity of the light (3 x 10^8 m s^{-1}).

$$AQY = \frac{6 \times \text{the no. of } CH_3OH \text{ molecules produced}}{\text{the no. of incident photons } (N_{photon})} \times 100$$

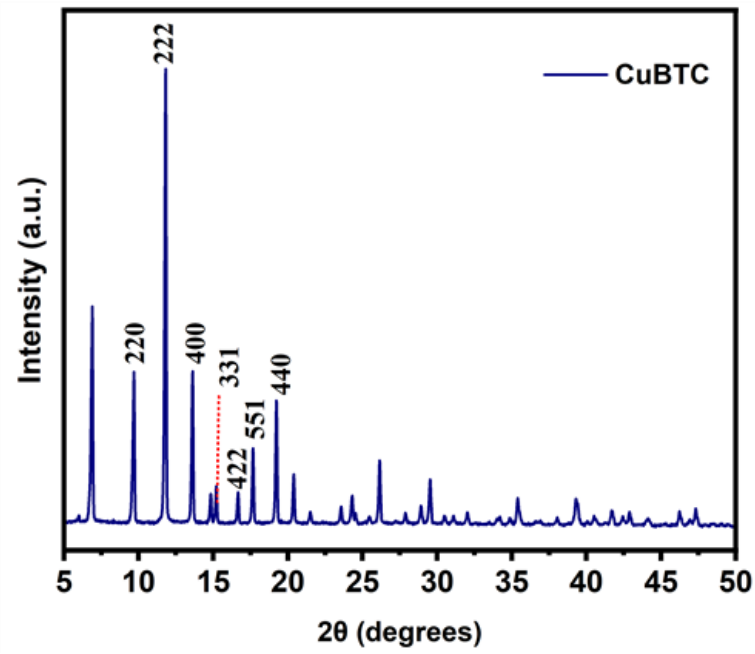

Figure S1. XRD pattern of CuBTC

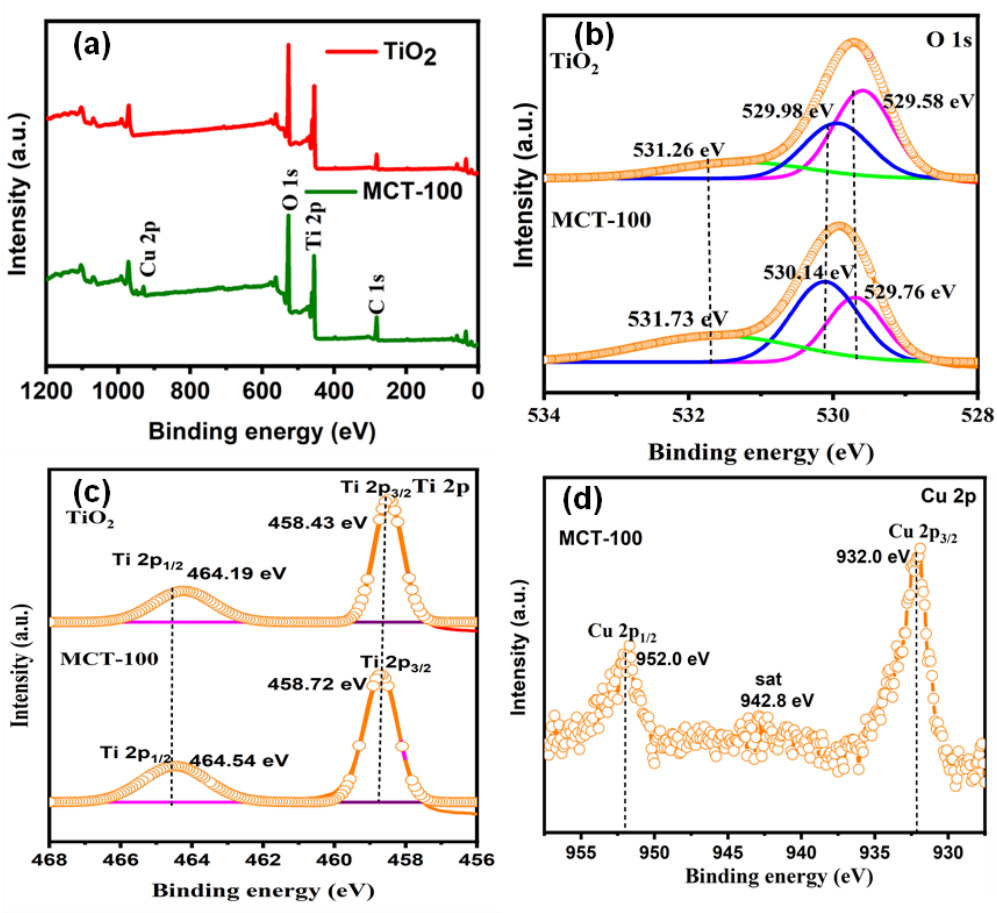

Figure S2. (a) Survey spectra of TiO_2 and MCT-100. XPS spectrum of (b) O1s (c) Ti 2p in TiO_2 and MCT-100. (d) XPS spectrum Cu 2p in MCT-100

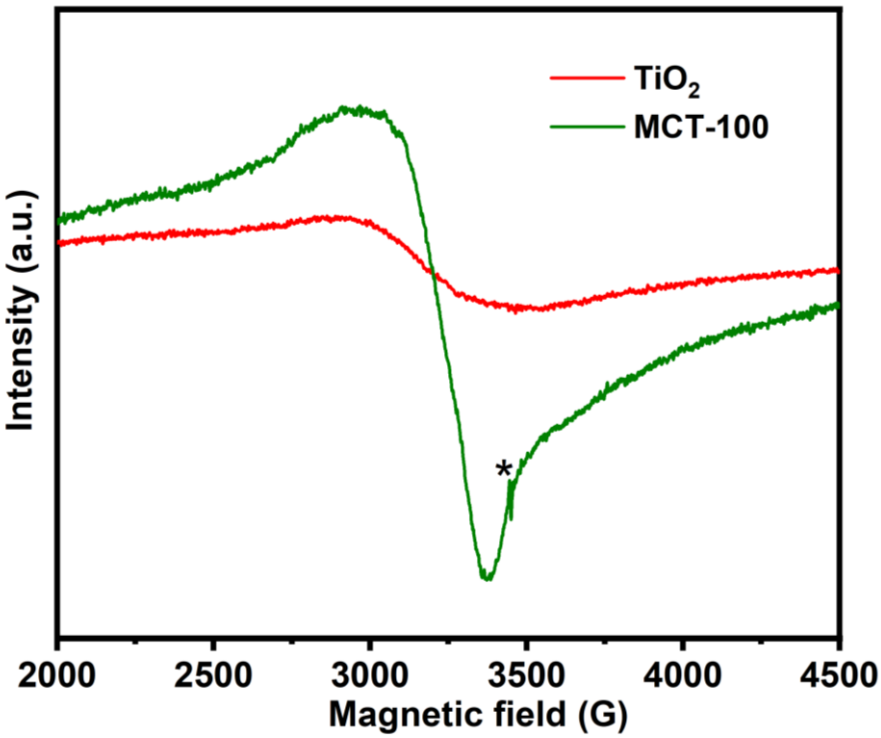

Figure S3. EPR spectrum of TiO_2 and MCT-100

The Electron paramagnetic Resonance (EPR) spectroscopy to identify paramagnetic species and to determine the oxidation states in TiO_2 and MCT-100. [3] The EPR spectrum of TiO_2 shows weak signals due to the paired electrons in Ti^{4+}, while MCT-100 reveals a significant peak at g=2.06, confirming the presence of Cu^{2+}.[4] A small but significant peak at g=1.99 indicates the presence of Ti^{3+} suggesting the formation of oxygen vacancies as shown in Fig.S3. These oxygen vacancies act as CO_2 adsorption sites and facilitate electron-hole separation, enhancing charge transfer, reducing recombination rates, and promoting the multi-electron reduction process necessary for converting CO_2 to methanol. [5]

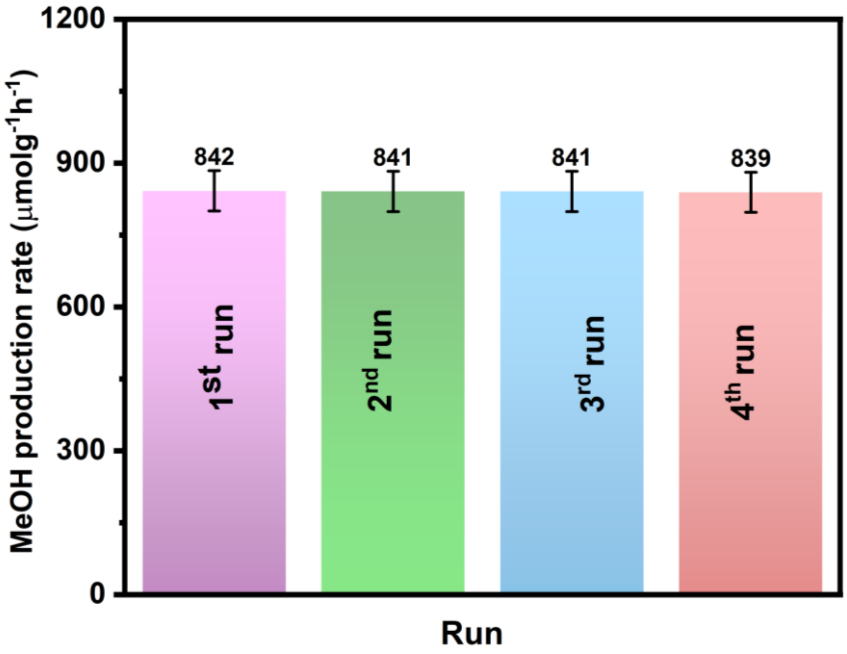

Figure S4. Recyclability test of the MCT-100 photocatalyst for methanol production

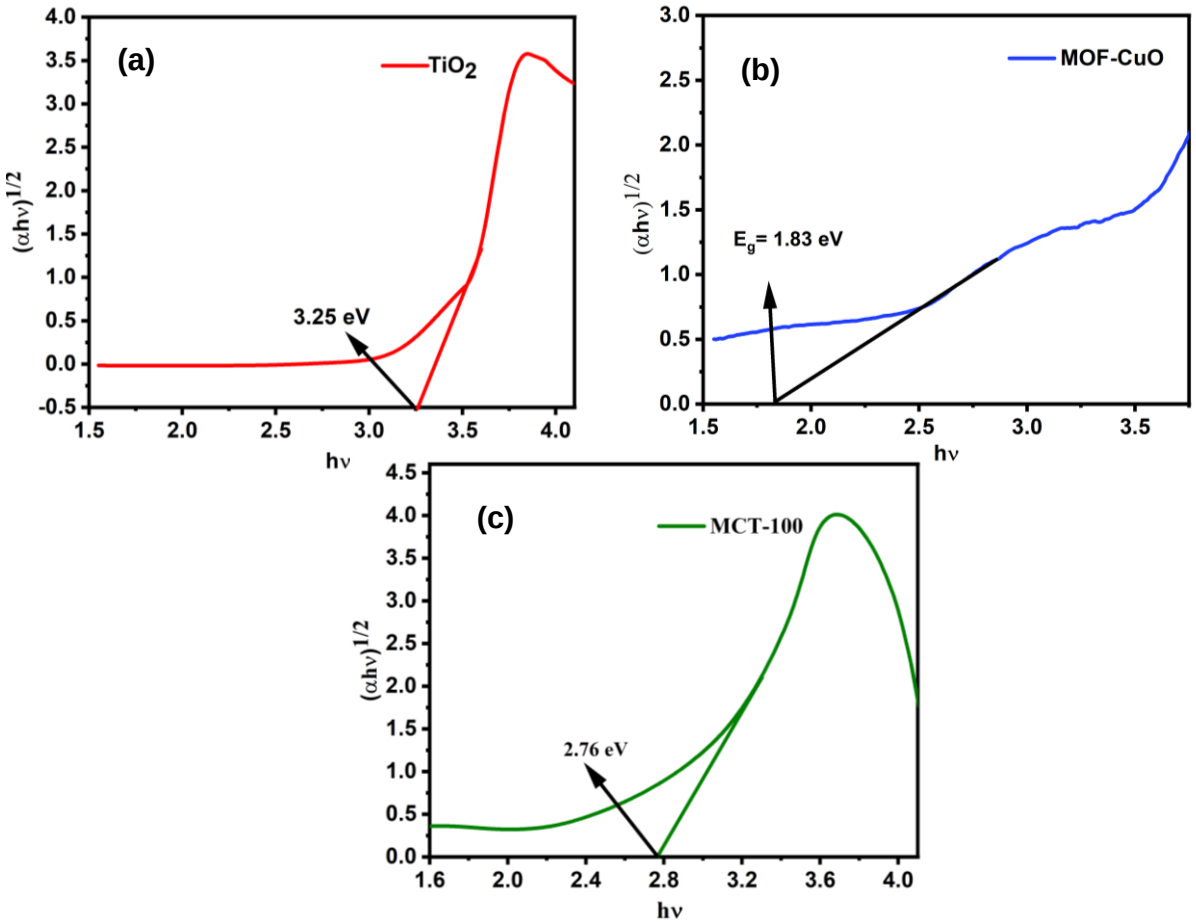

Figure S5 Tauc plots of (a) TiO_2 and (b) MOF-CuO (c) MCT-100

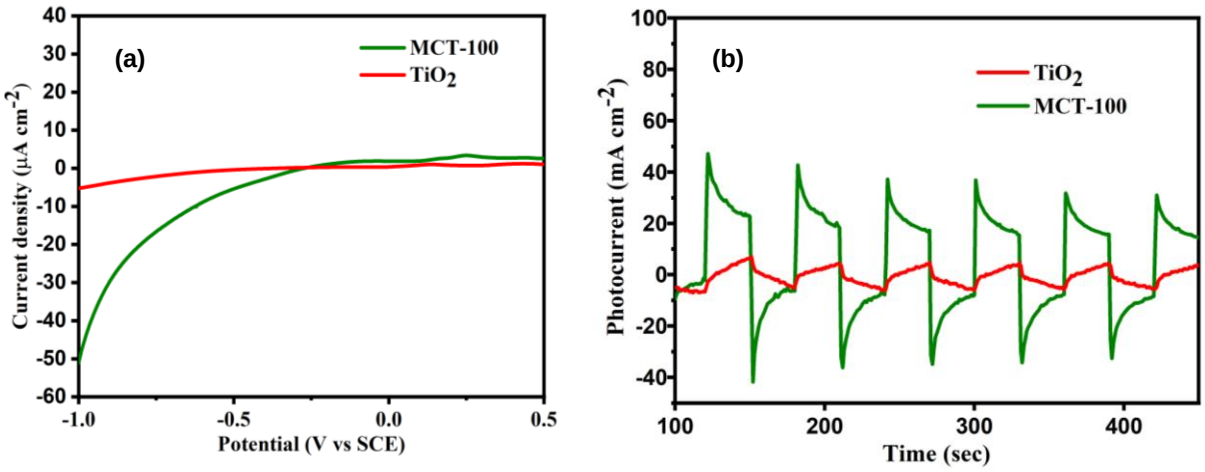

Figure S6. (a) Linear sweep voltammetry curves, and (b) transient photocurrent of TiO_2 and MCT-100

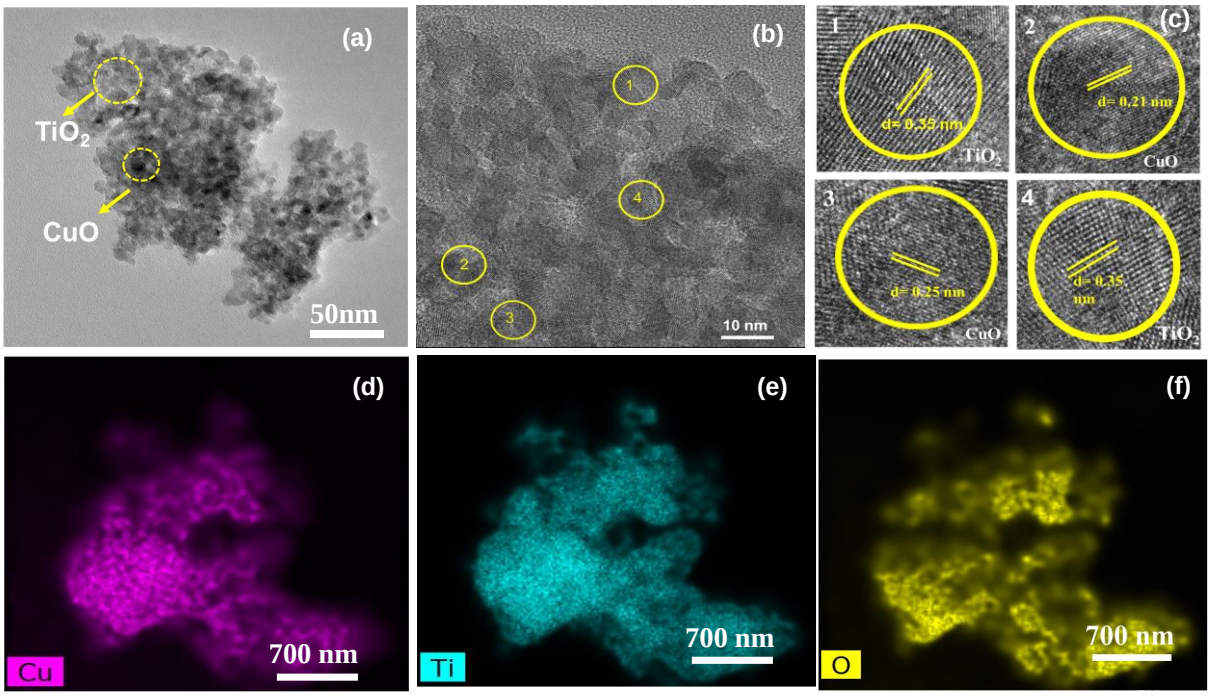

Figure S7. (a) TEM images MCT-100 (b)HRTEM images of MCT-100 (c) illustrates the lattice fringes of CuO and TiO_2. Elemental mapping (d) Cu (e) Ti and (f) O

The transition electron microscopy (TEM) revealed the formation of heterostructures in MCT-100 between TiO_2 and MOF derived CuO as shown in Fig.S7 a, b The d-spacings of 0.35nm corresponding to the (101) interplanar distances of anatase TiO_2, [6, 7]it could be observed clearly from the TEM images that Cu species enter into the lattice of TiO_2. CuO with d-spacing of 0.25 nm [8] and 0.21 nm for the plane (1 1 0) and (1 1 1), respectively can also be found at the surface of TiO_2 as shown in Fig.S7c. The elemental analysis of the MOF derived CuO/TiO_2 nanocomposite binary system was investigated. The Figure (S7 d, e, f) confirms the presence of copper (Cu), titanium (Ti), and oxygen (O) elements. The mappings of each element, depicted in clearly indicate that these Cu, Ti, and O species are uniformly distributed across the entire selected area. This uniform distribution demonstrates the continuous presence of oxygen within the CuO particle and TiO_2, extending through their interface. This portrayal effectively illustrates the establishment of a heterojunction between CuO and TiO_2, facilitating the transfer of charges between the bands of the two semiconductors.

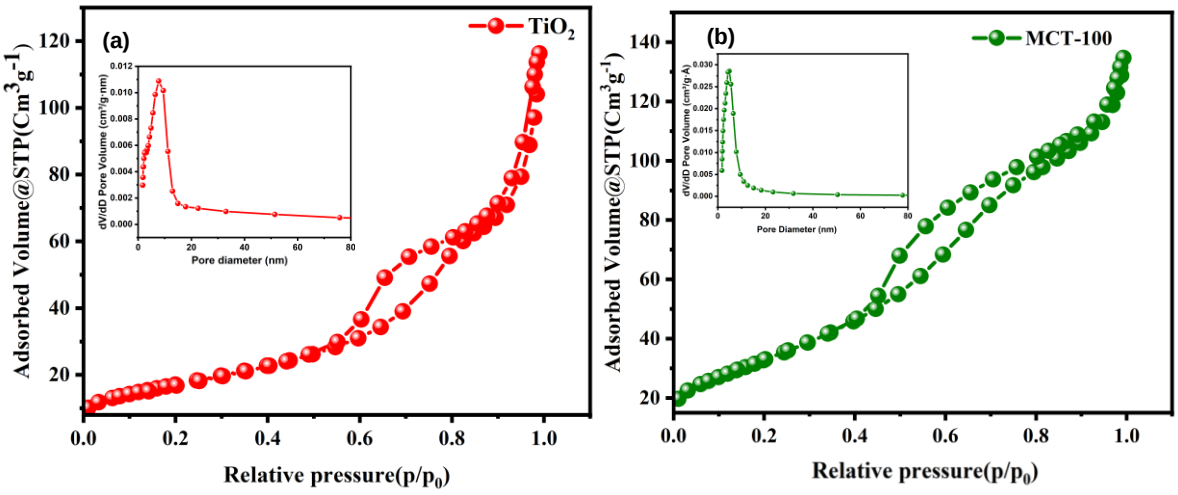

Figure S8. BET isotherms of (a) TiO_2 and (b) MCT-100

The porosity characteristics of both TiO_2 and MOF derived CuO (MCT-100) photocatalysts were assessed through nitrogen adsorption–desorption isotherms using BET and BJH techniques as shown in (Fig.S8 a, b). The calculated specific surface area (BET) values for TiO_2 and MOF derived CuO/TiO_2(MCT-100) are 62.12 m^2 g^{-1} and 122.11 m^2 g^{-1}. The MOF derived CuO on to the TiO_2 shows higher surface area. The specific surface area of a nanocomposite has a direct correlation with the surface-active sites, which have been found to be a controlling factor in photocatalytic activity. A hysteresis loop in the type-IV isotherm adsorption–desorption isotherm was observed at higher pressures, indicating the presence of mesopores.[9] Additionally, examination of the pore size distribution curve reveals that the average Barrett–Joyner–Halenda (BJH) pore diameters for TiO_2 and MCT-100 are 5.7 nm and 10.8 nm, respectively, suggesting that the as-prepared nanocomposites possess a mesoporous structure.

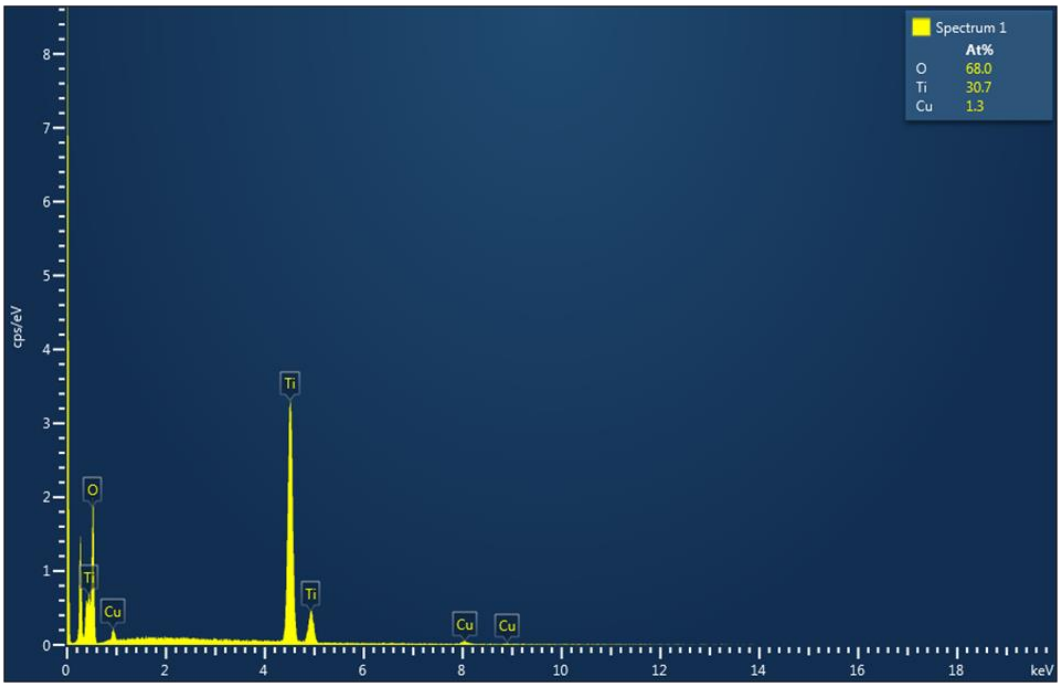

Figure S9. EDX pattern of MCT-100 showing copper is 1.3 at%

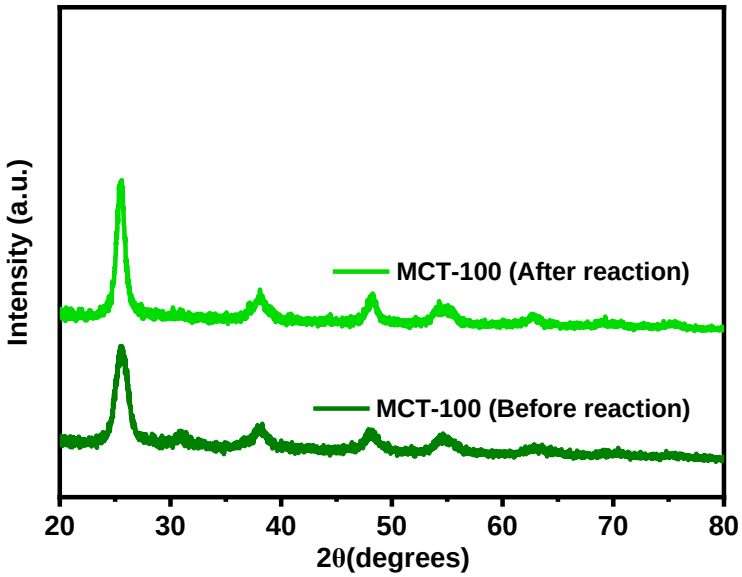

Figure S10. XRD pattern of MCT-100 before and after photocatalytic reaction in continuous flow

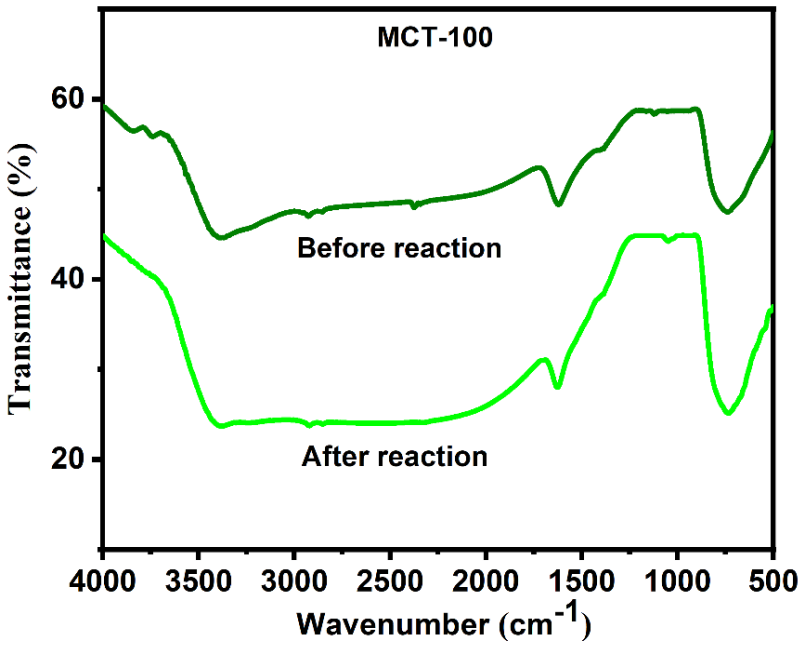

Figure S11. FTIR spectrum of MCT-100 before and after photocatalytic reaction in continuous flow.

To assess the catalyst's stability, XRD and FTIR studies were conducted on the catalyst samples before and after the photoreduction reaction. No changes in peak positions were observed in the XRD and FTIR patterns, (Fig S10, S11) indicating the catalyst remained stable throughout the reaction.

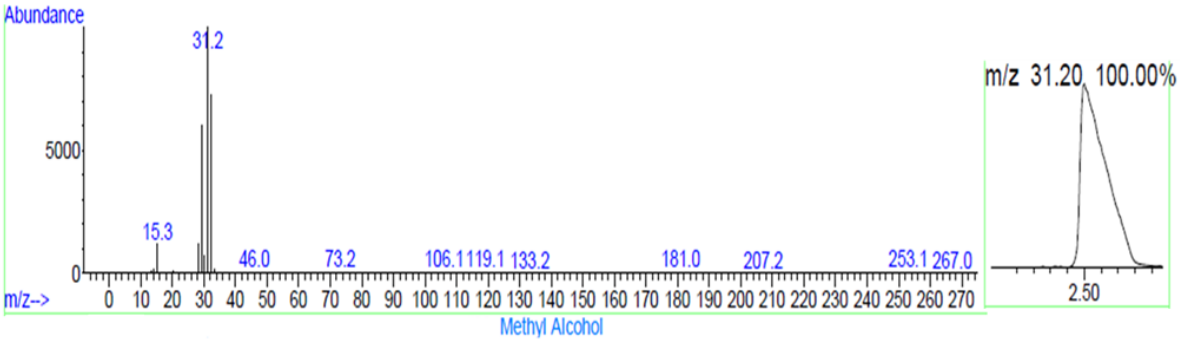

Figure S12. GC-MS chromatogram of reaction mixture showing m/z at 31.20 confirming the formation of methanol

Table S1. ICP-MS data of the photocatalysts

S.NO	Photocatalyst	Conc. [ppb] (Cu)
1	MCT-10	1286.6
2	MCT-50	7882.4
3	MCT-100	11293.9
4	MCT-200	25490.7

Table S2. Photocatalytic reduction of CO_2 into methanol using different photocatalysts

S. No	Catalyst	Reaction precursor	Cat (mg)	Visible-Light illumination	MeOH Rate ($\mu mol\ g^{-1}h^{-1}$)
1	None	CO_2	NIL	YES	NIL
2	TiO_2	CO_2	50	YES	64
3	MCT-10	CO_2	50	YES	541
4	MCT-50	CO_2	50	YES	702
5	MCT-100	CO_2	50	YES	842
6	MCT-100	N_2	50	YES	NIL
7	MCT-100	CO_2	50	NO	NIL
8	MCT-200	CO_2	50	YES	567

1.8 Photocatalytic methanol production through Flow mode with Auto-optimization.

Basic experimental setups for the photochemical auto-optimization platform.

1.8.1 Micro reactor system: A homemade PFA tubing (volume 1 mL; od 1.58 mm, id 1 mm, l = 1.3 meter) was fabricated as cartridge filled with 0.5 g of catalyst with molecular sieves shown in figure xx for the photochemically methanol production. The cylindrical reactor was placed for irradiation by a white light LED. The top of photochemical reactor was covered with aluminum foil to enhance light absorption.

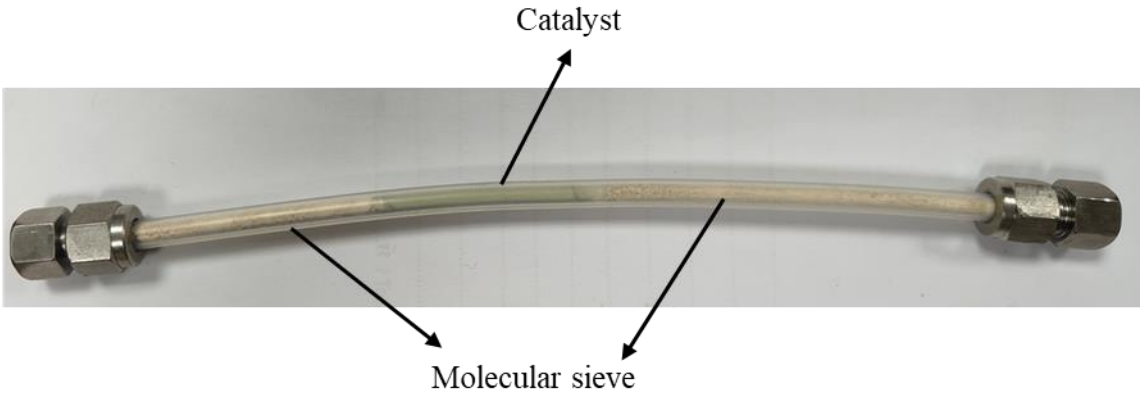

Figure S13. Manual designed photo-flow cartridge.

1.8.2 White LED reactor: We obtained a commercially available cylindrical-shaped 60W White LED (Figure S14a) for the photochemical reaction. We utilized a programmable power supply to control the lamp's power (in watts) by controlling the current and voltage (Figure. S14b). The power supply was connected to the central system through RS 232 to control the current and voltage.

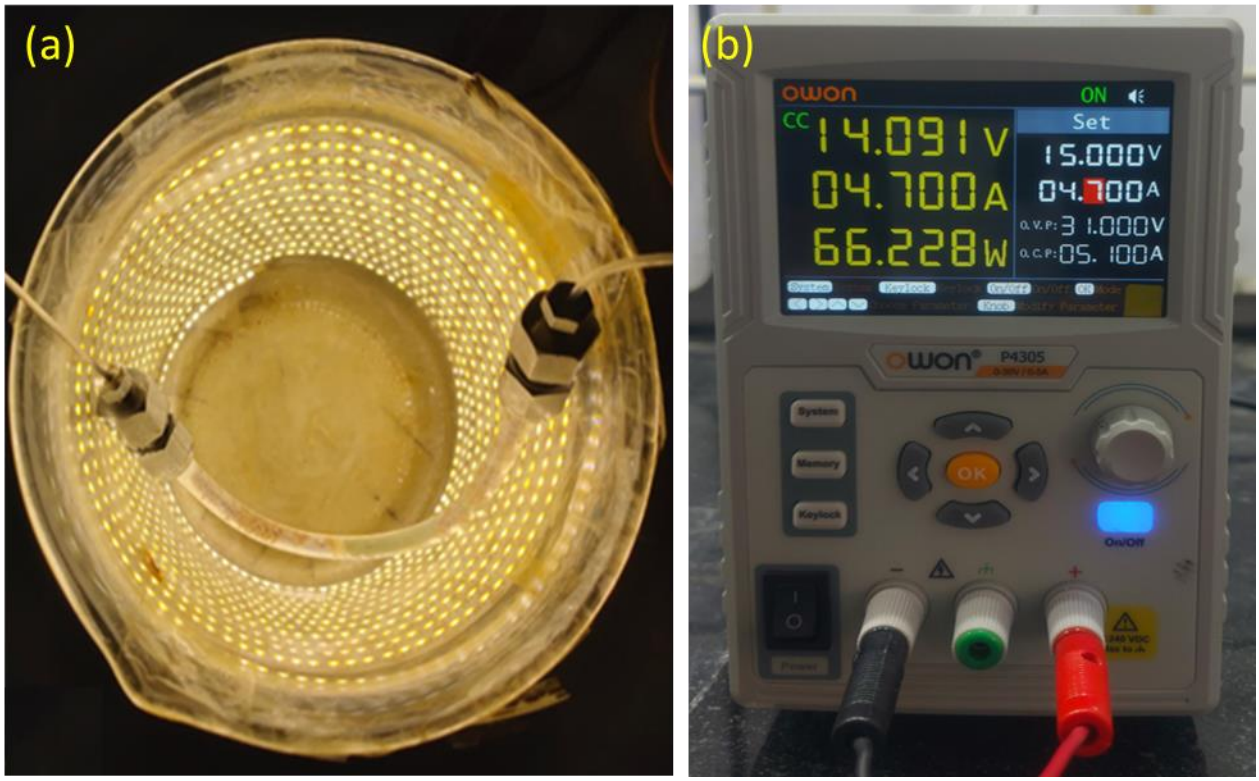

Figure S14. a) White LED light with PFA tubular cartridge filled with catalyst; (b) power supply.

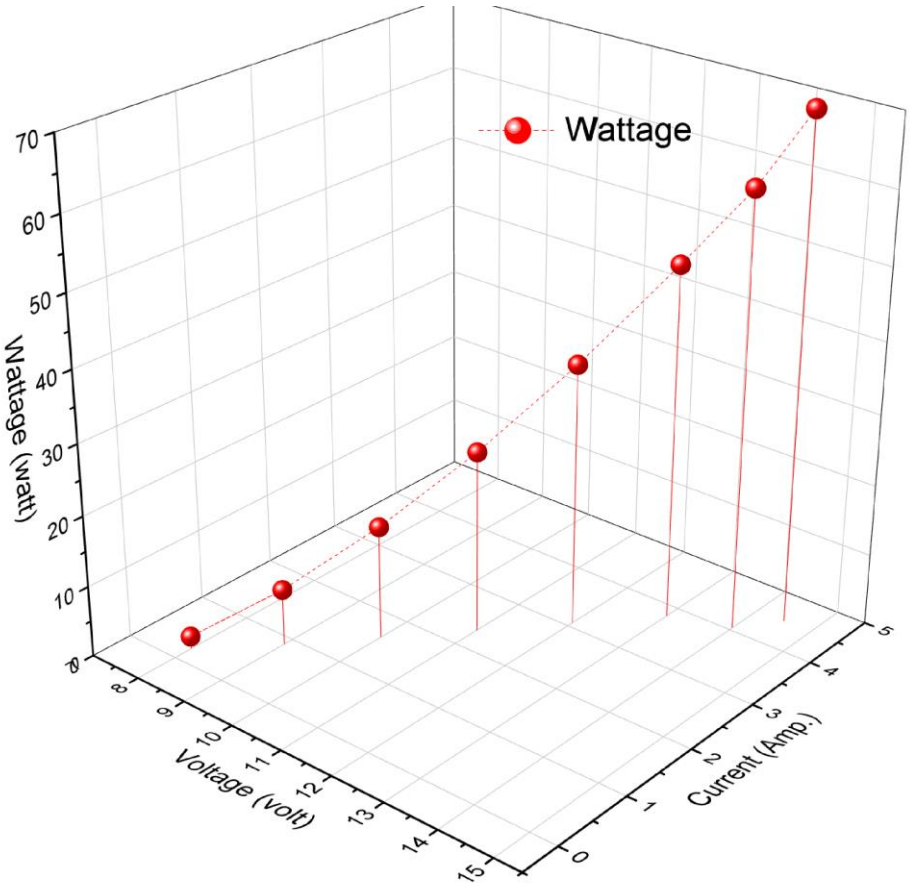

Figure S15. 3D graph of the relation between voltage (V), current (Amp) and white light intensity (W).

1.8.3 Pumps: The Syringe pump were directly connected to the main computer via an RS-232 interface. These S10 pumps introduced reactant solutions into the PFA cartridge at the central computer's prescribed flow rate (Figure S16), and the flow rate of CO_2 gas was controlled with micro flow controller (MFC) which is connected to main computer system via COM. To convey information regarding the flow rate, operational status, and duration, serial communication utilizing ASCII code was employed between the central computer and the syringe pump. This allowed the main computer to transmit the necessary details to the pumps, enabling them to initiate their operations accordingly.

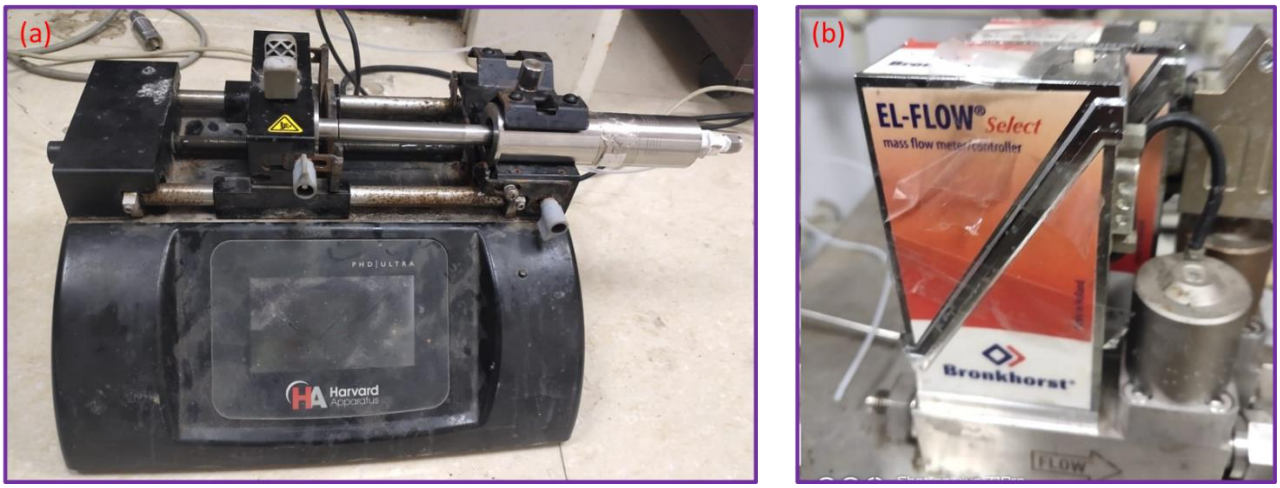

Figure S16. Actual Picture of working syringe pump and Mass flow controller

1.8.4 Auto-collector: We utilized a commercially available 3D printer for the auto-sampler as reported in one paper. The Python program on the central computer interfaced with the 3D printer. The Python program commanded the 3D printer to rotate, and this information was communicated to USB serial communication. This setup allowed us to control the 3D printer for tasks such as sample collection, reactor stabilization, and washing in various situations (Figure. S17).

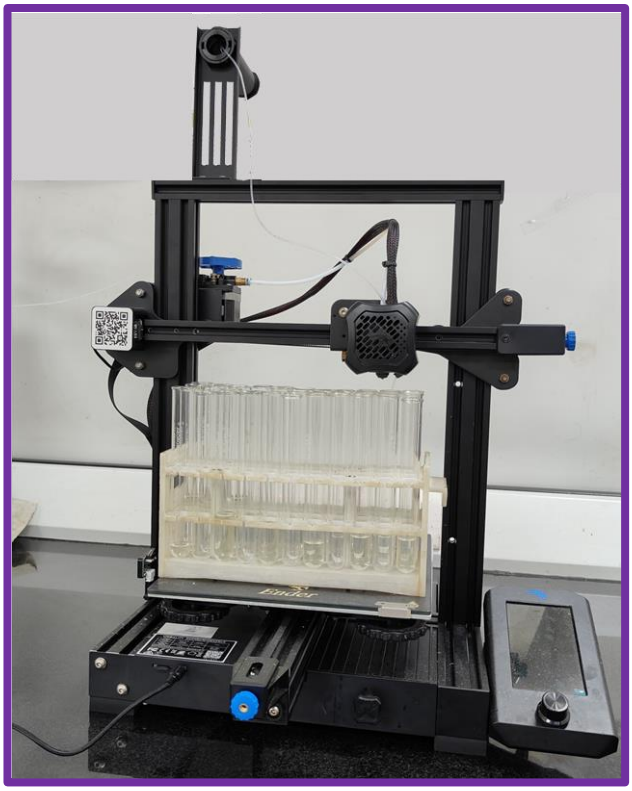

Figure S17. Actual photograph of 3D printer as auto-fraction collector.

1.8.5 Auto-optimized reactor system: We have all accessories like pumps, LED light reactor, Owon power supply, and 3D printer connected to the central computer system with RS 232 and USB cable. We have made a combined program including Bayesian optimization for automatically changing the parameters such as flow rate and power of irradiation of white light to maximize yield.

1.8.6 Bayesian optimization algorithm.

The Bayesian optimization algorithm used in this platform was a modified version of a meta-optimizer (MO) algorithm consisting of multiple surrogate models and a single acquisition function. The surrogate models used in this algorithm were similar to the original reported one, and the surrogate model was selected as an expected improvement. To proceed with the optimization process, the Sobol algorithm was chosen to generate the initial point before the commencement of the main Bayesian optimization loop for 3 consecutive rounds. Then, the meta-optimizer loop was started to maximize the reaction build (Figure. S18).

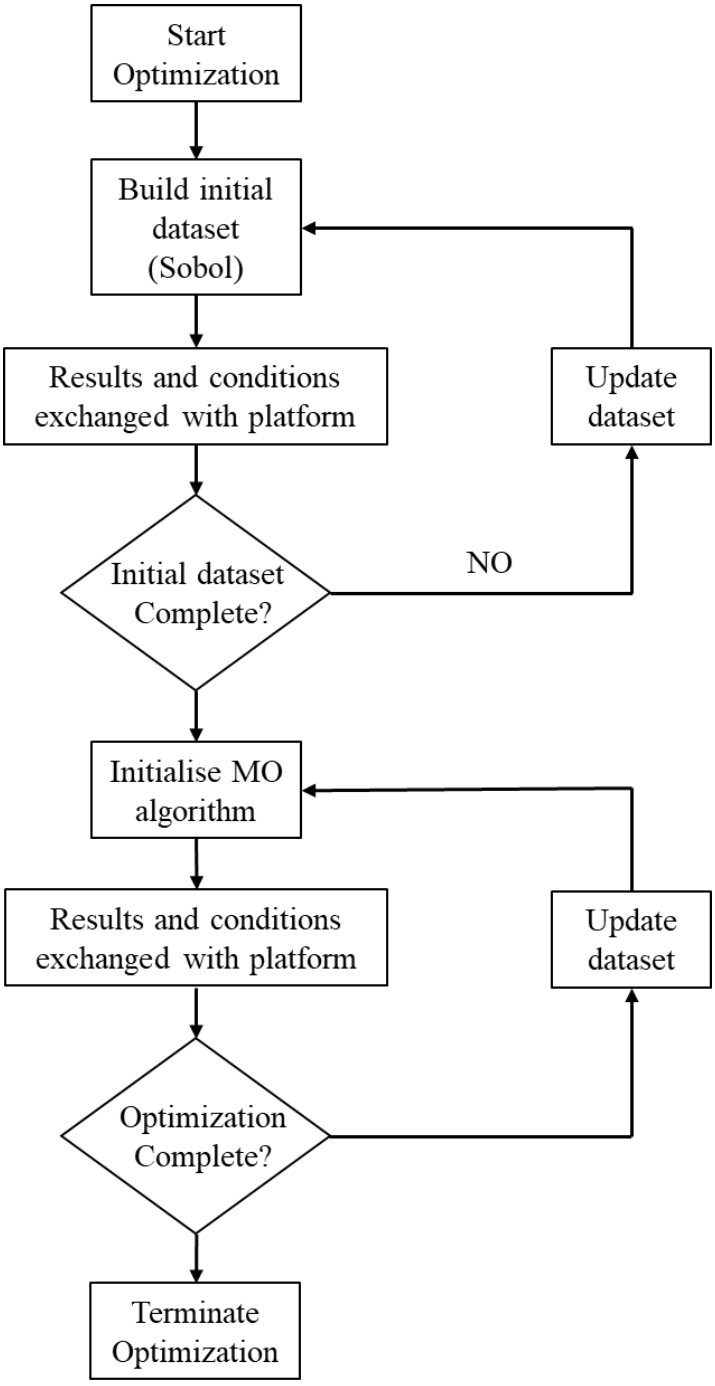

Figure S18. Algorithm flow chart of user-planning mode with two variables in the auto-optimization.

1.9 Experimental design via Bayesian optimization (BO) for the photo flow methanol production.

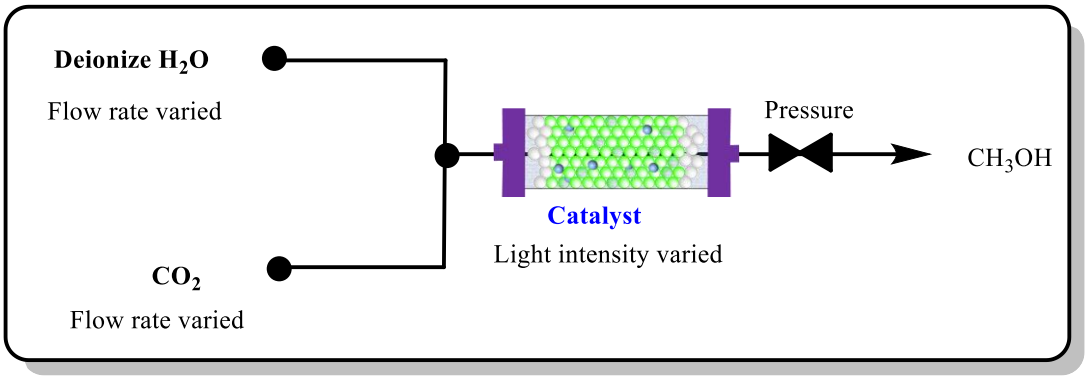

The syringe pumps and MFC were manipulated as programmed in the central computer to inject and control the flow rates of the two respective solutions comprising deionize water and CO_2 gas. Both solutions were introduced through a T-mixer at varied flow rate (Q) and then passed through a PFA cartridge (od = 1/4, id = 4 mm, l = 0.21 m, vol. = 1mL) filled with catalyst exposed to various white light intensity (W) exposure. The top of photochemical reactor was covered with aluminium foil to enhance light absorption. The resulting solution after passing through PFA cartridge under pressure and collected in our previously reported auto-collector. Bayesian optimizer (BO) will present the following values for the variable flow rate and white light (W). In this optimization, analysis is done out-station with GC-FID for methanol detection for every fraction which is collected. After running first condition given by BO we need to write the yield.

Python Code

rc.py*

```python
from os import listdir
from os.path import isfile, join
import serial

import numpy as np
import pandas as pd
import time


import propar

#step1: be sure to the address of the files that the ftir data is exported is matching to line 11 (mypath)
#mypath = "abhilash\\soft\\test mfc code\\Dummy Data"

mypath="C:\\Users\\Dr.AJAY K SINGH\\Desktop\\RUCHI\\23-04-2024"



onlyfiles = [f for f in listdir(mypath) if isfile(join(mypath, f))]


#step2: make sure that pump and the potentiostat is correctly addressed in the line 16 and 17
pump_1 = serial.Serial("COM13",9600) #HPLC Pump
port = serial.Serial("COM1",115200)
printer = serial.Serial("COM14", 115200, timeout=1)
MFC = propar.instrument('COM8')
port = serial.Serial("COM7",115200) #power_supply

def gas_flow(set_val):

   MFC.writeParameter(206, set_val)


def valve_reset():
    #run if valve is refusing to close, i.e. in forced full open mode

    MFC.writeParameter(12, 0)

    return "valve was reset"


def function(flowrate_1,flow_g,v,i,time_hold):

     #set the pumps with the flowrate as the desired flowrate for the function


    fr_1 = flowrate_1*1000   #ml/min
    pump_1.write(('flow:'+ str(fr_1) + '\r').encode())
    time.sleep(0.1)

```

```python
    #pumps run
    pump_1.write(b'on\r')
    time.sleep(0.1)
    gas_flow(flow_g)

    vol = v
    curr = i
    port.write(('VOLT '+str(vol)+'\r\n').encode())     #to change the voltge we need to use "VOLT 1" command
    port.write(('CURR '+str(curr)+'\r\n').encode())    #to change the current we need to use "CURR 1" command

    time.sleep(0.1)

    time.sleep(time_hold)

#step 4:grab the line 93 and f9
from skopt.optimizer import Optimizer


#step5:in line 96 we have to define the range that (flowrate,flow_gas) (from,to) and after (anytime) appllying changes you need to grab the line 96 and f9
#flowrates are in ml/min
bounds = [(0.1,0.5),(10,30),(12.5,14.5),(4.9,5.0)]
#step 6: grab the line 100 and f9
opter =Optimizer(bounds,base_estimator='gp',n_initial_points=3,acq_func="EI",random_state=np.random.randint(3326))


#step7: to selecte number of the cycles that you have to do the experiment and then grab the line 104 to 121 and f9: the closed loop experimentation is initiated
number_of_cycles =22
results = []
flowrates_1 = []
flow_g = []
vs = []
currents = []


product_percentage=True #set to true if product wavelengths being monitored

if product_percentage == True:
    val=1
else:
    val=-1


# Step 8: Test Tubes on Printer
USE_PRINTER = True
REST_HEIGHT = 200
X_HOME = -5
Y_HOME = 20
Z_HOME = 175
DEFAULT_PUMP_TIME="1"
# Distance between test tubes
X_SPACING=20
Y_SPACING=20
# Number of test tubes
```

```
X_ROWS = 11
Y_COLUMNS = 4

def send_cmd(cmd):
    print(cmd)
    printer.write(f"{cmd}\n".encode("ASCII"))

def move(x=None, y=None, z=None):
    s = "G0"
    if x is not None:
        s += f"X{x}"
    if y is not None:
        s += f"Y{y}"
    if z is not None:
        s += f"Z{z}"

    s+= "F5000"
    send_cmd(s)

def printer_positions():
    for j in range(Y_COLUMNS):
        for i in range(X_ROWS):
            if j%2==1:
                yield (X_HOME + (X_ROWS - 1 - i) * X_SPACING, Y_HOME + j * Y_SPACING, Z_HOME)
            else:
                yield (X_HOME + i * X_SPACING, Y_HOME + j * Y_SPACING, Z_HOME)

# Run this.
tube_location = list(printer_positions())
```

```
try:
    valve_reset()
    for i in range(number_of_cycles):
        move(*tube_location[2*i])
        asked = opter.ask()
        print(asked[0])
        print(asked[1])
        print(asked[2])
        print(asked[3])

        time_hold_reaction=800#time for each run

        function(asked[0],asked[1],asked[2],asked[3],time_hold_reaction)
        move(*tube_location[2*i+1])

        #hplc input value

        time.sleep(1300) #for collection in 2nd test tubeA
        function(0,0,0.01,0.001,0) #turns off pump and power supply

        offline_told = float(input("give the results from offline analysis\n"))
        opter.tell(asked,offline_told*(-val))

        results.append(offline_told)
        flowrates_1.append(asked[0])
        flow_g.append(asked[1])

        dict1 = {"flowrate_1":flowrates_1,"flow_g":flow_g,"area-results":results}
        df2 = pd.DataFrame(dict1)
        df2.to_csv("output round "+str(i)+".csv")
finally:
    pump_1.write(b'off\r')
    gas_flow(0)
```

Table S3. Photo-flow auto-optimization reaction parameters boundary of methanol production

Parameters	Flow rates of water (mL/min.)	Flow rates of gas (mL/min.)	Volage (volt)	Current (amp)	Light Power (watt)
Boundary	0.1-0.5	10-50	12.5-14.5	4.9-5	43-68

General procedure for the auto-optimized production of methanol.

In our approach we are employing a python-coded based Bayesian optimization strategy for further refinement. Initial steps involved to check all the pumps, white LED and 3D printer connected to computer system and then filled the deionize water in one syringe and connected to a syringe pump on other hand MFC was connected to CO_2 gas cylinder. Both gas and deionize water mixing at T-mixer and resulting solutions were then directed through a PFA tubular cartridge (inner diameter = 4 mm, length = 0.21 m, volume = 2.6 mL, filled with 0.5 g of catalyst, free volume 1 mL) surrounded by a cylindrical-shaped white LED light source under 10 bar pressure. Once the solution setup was complete, input ranges for variable flow rates, voltages, and current were specified in the Python code designed for the reaction. The Bayesian optimizer systematically explored these varying reaction conditions, aiming to achieve maximum yield. The optimization process involved running 22 experiments, analysis is done outstation utilizing GC-FID and the results were tabulated in the optimization table (Table.S4).

Table S4. Auto-optimization table of photo-flow methanol production.

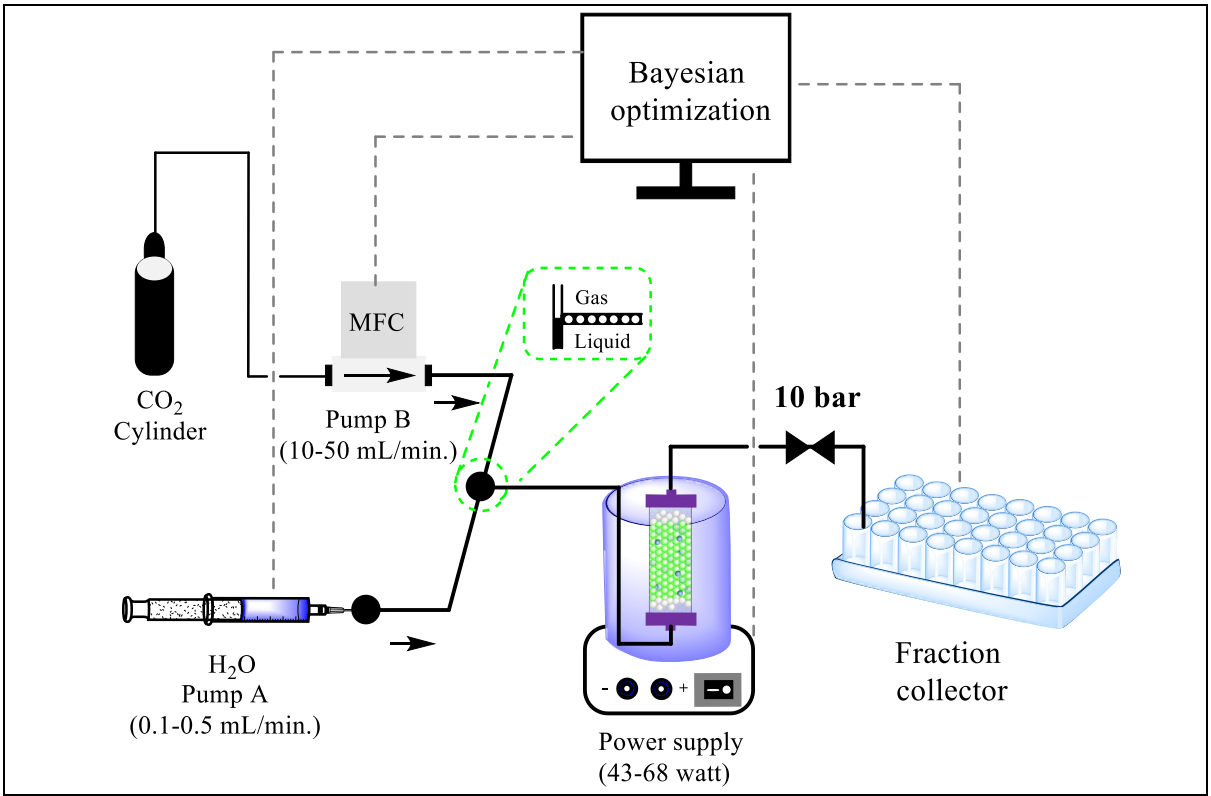

Entry	Flow Rate (mL/min.)		Voltage (V)	Light intensity (W)	Residence time (sec)	Moles of MeOH formed mol $g^{-1}h^{-1}$
	deionize water	CO_2 gas				
1	0.24	24	12.81	46.12	2.5	0.116568611
2	0.13	13	12.58	43.14	4.6	0.070892019
3	0.1	15	14.5	68.77	4	0.676545398
4	0.1	10	14.5	52.25	5.9	0.404331332
5	0.12	15	14.09	62.15	4	0.696583887
6	0.5	30	13.12	50.02	2	0.154446178
7	**0.26**	**22**	**14**	**63.45**	2.7	**2.346144413**
8	0.39	23	12.55	43.61	2.6	0.101103029
9	0.21	18	14.17	63.32	3.3	2.246529794
10	0.12	15	14.3	64.8	4	0.918521272
11	0.16	17	13.67	56.34	3.5	0.335836563
12	0.16	22	13.67	56.34	2.7	0.508502109
13	0.5	12	13.16	49.95	4.8	1.006162789
14	0.27	20	13.98	60.64	3	1.777769094

15	0.12	20	12.83	45.79	3	0.045950049
16	0.1	25	13.05	48.74	2.4	0.16079856
17	0.16	27	13.67	56.61	2.2	0.483087402
18	0.16	13	14	62.14	4.6	1.062181469
19	0.33	15	12.58	42.92	3.9	0.073079654
20	0.11	20	14	61.99	3	0.648112386
21	0.4	19	14.2	64.67	3.1	2.271185119
22	0.5	30	13.16	49.66	2	0.075873755

Reaction condition: 10 bar pressure, od = ¼; id = 4 mm; volume = 2.6 mL PFA cartridge filled with 0.5 g of catalyst and molecular sieves with 1 mL free space.

Table S5. Calculation of rate of production of methanol

Entry	Reference volume (μL)	Reference area	Experimental area	Ratio	Moles of MeOH	Cu amount per g catalyst	Flow rate (μl/min.)	Liquid coming out in 1 h	Moles of MeOH formed (mol h^{-1})	Moles of MeOH formed (mol $g^{-1}h^{-1}$)
1	10	500000	832.32	0.00166464	5.19388E-08	0.0065	243.13721	14588.23285	0.000757696	0.116568611
2	10	500000	949.87	0.00189974	5.92743E-08	0.0065	129.56665	7774.000589	0.000460798	0.070892019
3	10	500000	11745.11	0.02349022	7.32924E-07	0.0065	100	6000	0.004397545	0.676545398
4	10	500000	7019.3604	0.01403872	4.38026E-07	0.0065	100	6000	0.002628154	0.404331332
5	10	500000	10032.26	0.02006452	6.26038E-07	0.0065	120.541	7232.46	0.004527795	0.696583887
6	10	500000	536.25	0.0010725	3.34633E-08	0.0065	500	30000	0.0010039	0.154446178
7	10	500000	15630.3	0.0312606	9.7537E-07	0.0065	260.58352	15635.03371	0.015249939	2.346144413
8	10	500000	447.61	0.00089522	2.7932E-08	0.0065	392.12004	23527.50003	0.00065717	0.101103029
9	10	500000	18608	0.037216	1.16119E-06	0.0065	209.591	12575.46	0.014602444	2.246529794
10	10	500000	13288.26	0.02657652	8.29221E-07	0.0065	120	7200	0.005970388	0.918521272
11	10	500000	3632.81	0.00726562	2.26696E-07	0.0065	160.48614	9629.343685	0.002182938	0.335836563
12	10	500000	5593.79	0.01118758	3.49066E-07	0.0065	157.81422	9468.866531	0.003305264	0.508502109
13	10	500000	3514.02	0.00702804	2.19284E-07	0.0065	497.07705	29824.65423	0.006540058	1.006162789
14	10	500000	11255.65	0.0225113	7.02381E-07	0.0065	274.1984	16451.904	0.011555499	1.777769094
15	10	500000	664.76	0.00132952	4.14827E-08	0.0065	120	7200	0.000298675	0.045950049
16	10	500000	2791.53	0.00558306	1.74198E-07	0.0065	100	6000	0.001045191	0.16079856

17	10	500000	5184.69	0.01036938	3.23538E-07	0.0065	161.75691	9705.419526	0.003140068	0.483087402
18	10	500000	11844.02	0.02368804	7.39096E-07	0.0065	155.68966	9341.378796	0.00690418	1.062181469
19	10	500000	379.75	0.0007595	2.36973E-08	0.0065	334.08687	20045.18632	0.000475018	0.073079654
20	10	500000	10576.7	0.0211534	6.60012E-07	0.0065	106.38072	6382.804318	0.004212731	0.648112386
21	10	500000	9857.18	0.01971436	6.15113E-07	0.0065	400	24000	0.014762703	2.271185119
22	10	500000	263.44	0.00052688	1.64393E-08	0.0065	500	30000	0.000493179	0.075873755

Graphs

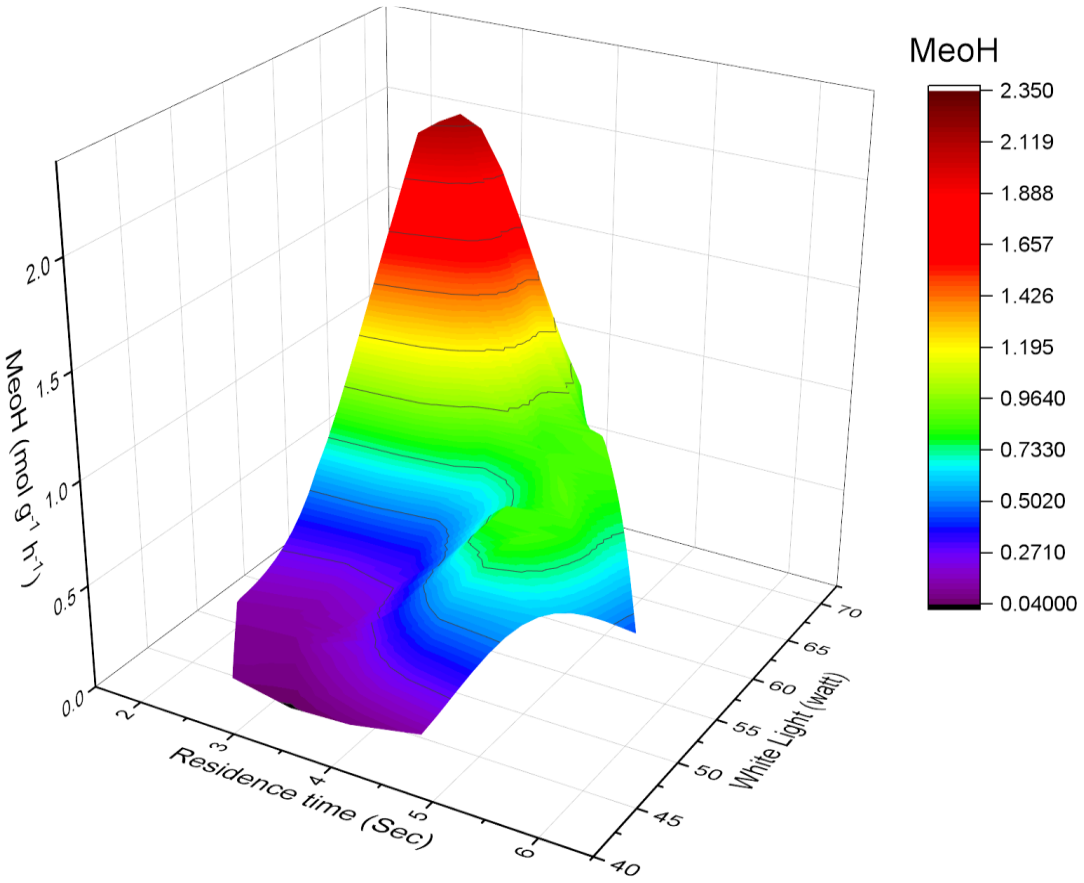

Figure S19. AI based system to auto-optimize and navigate this complexity and identify the optimal conditions for the photo activated methanol production.

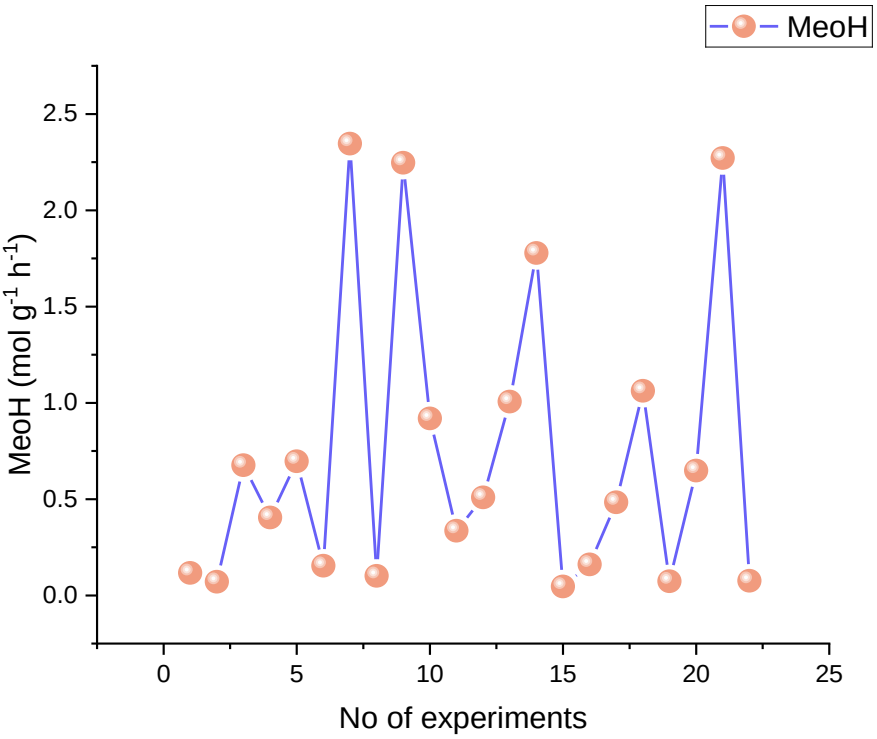

Figure S20. 2D graph between no of experiments performed versus yield obtained through AI based auto-optimization for the production of methanol.

General procedure of running AI-optimized condition for longer time for the production of methanol.

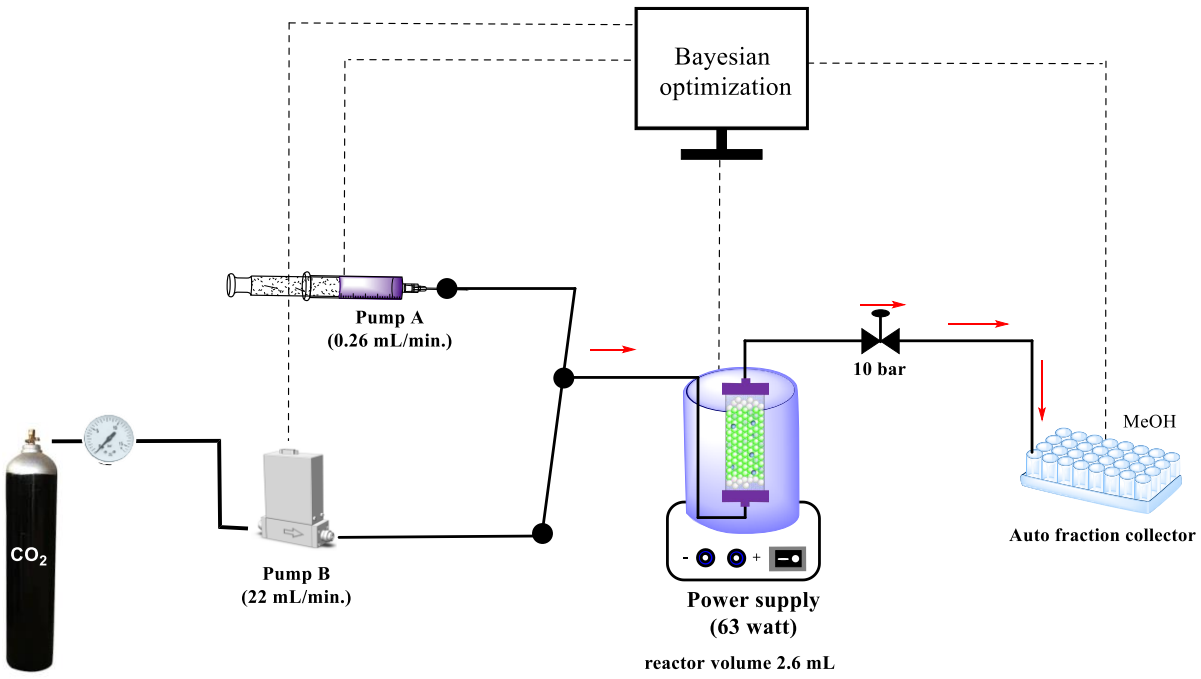

Figure S21. Schematic presentation of **AI integrated** continuous flow for the **production of methanol**.

The stock solution of deionized water was charged in one syringe, and carbon dioxide gas were introduced into the microreactor with a T-mixer using two separate pumps. The flow rate of the deionized water was kept 0.26 mL/min. and flow rate of carbon dioxide gas was maintained at 22 mL/min.The resulting solutions were introduced to a T-mixer and then passed through a PFA tube (od = ¼; id = 4 mm; volume = 2.6 mL) filled with 0.5 g of CuO/TiO_2 with 1mL free space, under white light (63 W) exposure to occur the methanol production during 2.7 sec. of residence time at room temperature and 10 bar pressure. The out-put of the reactor was connected with spring based back pressure regulator (~10 bar) to maintain the flow of gas Then out coming first one hour of the methanol was discarded and next 5 h of the product methanol 0.075 mol/5h was collected in HPLC bottle.

Quantum efficiency (ϕ) calculation:

The values of the number of incident photons ($N_{photons}$) were calculated using the following equations. Here,

$$N_{\text{photon}} = \frac{P\lambda t}{hc}$$

Power of the light (p) = 63 W = 63 $J\ s^{-1}$

λ = Wavelength of the light (400 nm) = 400 x 10^{-9} m

t = Duration of irradiation time, 5 h = 18000 s,

h = Planck's constant = 6.626 x 10^{-34} J s

c = Velocity of light = 3 x 10^{8} m s^{-1}

No of photons incident

$$N_{\text{photon}} = \frac{63\ \text{J s}^{-1} \times 400 \times 10^{-9}\ \text{m} \times 18000\ s}{6.626 \times 10^{-34}\ \text{J s} \times 3 \times 10^{8}\ \text{m s}^{-1}}$$

$$N_{\text{photon}} = 2.3 \times 10^{24}$$

$$Mole's\ photons\ incident = \frac{N_{\text{photon}}}{N}$$

[N = Avogadro's number (6.02214×10^{23})]

$$Mole's\ photons\ incident = \frac{2.3 \times 10^{24}}{6.02214 \times 10^{23}}$$

$$Mole's\ photons\ incident = 3.82\ mole$$

Moles of product formed in 5h:

$$Mole's\ of\ product\ formed = 7.5 \times 10^{-2}$$

Quantum efficiency (ϕ):

$$\text{Quantum efficiency } (\emptyset): = \frac{Mole's\ of\ product\ formed}{Mole's\ photons\ incident} \times 100$$

$$\text{Quantum efficiency } (\emptyset): = \frac{7.5 \times 10^{-2}}{3.82} \times 100$$

$$\text{Quantum efficiency } (\emptyset): = 2.0\ \%$$

Quantum efficiency (ϕ) calculation:

The values of the number of incident photons ($N_{photons}$) were calculated using the following equations. Here,

$$N_{\text{photon}} = \frac{P\lambda t}{hc}$$

Power of the light (p) = 63 W = 63 $J\ s^{-1}$

λ = Wavelength of the light (400 nm) = 700 x 10^{-9} m

t = Duration of irradiation time, 5 h = 18000 s,

h = Planck's constant = 6.626 x 10^{-34} J s

c = Velocity of light = 3 x 10^{8} m s^{-1}

No of photons incident

$$N_{\text{photon}} = \frac{63\ \text{J s}^{-1}\ \times 700 \times\ 10^{-9}\ \text{m}\ \times 18000\ s}{6.626\ \times\ 10^{-34}\ \text{J s} \times\ 3 \times 10^{8}\ \text{m s}^{-1}}$$

$$N_{\text{photon}} =\ 4.0\ \times 10^{24}$$

$$Mole's\ photons\ incident\ = \frac{N_{\text{photon}}}{N}$$

[N = Avogadro's number (6.02214×10^{23})]

$$Mole's\ photons\ incident = \frac{4.0\ \times 10^{24}}{6.02214 \times\ 10^{23}}$$

$$Mole's\ photons\ incident\ = 6.64\ mole$$

Moles of product formed in 5h:

$$Mole's\ of\ product\ formed\ = 7.5\ \times 10^{-2}$$

Quantum efficiency (ϕ):

$$\text{Quantum efficiency } (\emptyset): = \frac{Mole's\ of\ product\ formed}{Mole's\ photons\ incident} \times 100$$

$$\text{Quantum efficiency } (\emptyset): = \frac{7.5\ \times 10^{-2}}{6.64}\ \times 100$$

$$\text{Quantum efficiency } (\emptyset): = 1.1\ \%$$

Table S6: Comparison table for photocatalytic methanol production

S.No	Catalyst	Light source	Solvent	Methanol production rate	Reference
1.	POM@TiO_2	Xe lamp (100 $mW.cm^{-2}$).	5 mL ultrapure water	21 µmol g^{-1} h^{-1}	[7]
2.	2.5%Ag/TiO_2	UV and visible light irradiation (λ>400 nm).	Water	135.06 µmol g^{-1} h^{-1}	[10]
3.	T120	solar light (λ > 200 nm)	$NaHO_3$	9.1 µmol$g^{-1}h^{-1}$	[11]

4.	CD/FAT	300 W Xenon lamp	Water	24.2 µmol g^{-1} h^{-1}	[12]
5.	0.5% Cu_1@BiOBr	300 W Xenon lamp	water	627.66 µmol $g^{-1}h^{-1}$	[13]
6.	$STCu_{0.08}$-H	300 W xenon lamp	water	5.38±0.19 µmol $g^{-1}h^{-1}$	[14]
7.	4%Ni/TiO_2	60 W-UV light	water	90.81 µmol $g^{-1}h^{-1}$	[15]
8.	$ZnFe_2O_4$/TiO_2	500 W xenon lamp	Water /Na_2S, Na_2SO_3, /KOH	27.78µmol g^{-1} h^{-1}	[16]
9.	23.2%AgBr/TiO_2	150W Xe lamp	Water/ 0.2 M $KHCO_3$	15.57 µmol $g^{-1}h^{-1}$	[17]
10.	$Ru(bpy)_3$/TiO_2	20W LED	Water /DMF / TEA	78.16 µmol $g^{-1}h^{-1}$	[18]
11.	CeF_3/TiO_2	500 W Xenon lamp	Water	54.06 µmol $g^{-1}h^{-1}$	[19]
12.	Cu_2O	300 W Xe lamp	Ultrapure deionized H_2O	1.2*10^6 µmol g^{-1} h^{-1}	[20]
13	**MCT-100**	**420 W Xe lamp**	**DMF/Deionised H_2O**	**842 µmol g^{-1} h^{-1}**	**This work**
14*	**MCT-100**	**White LED**	**Deionised H_2O**	**2.3 *10^6 µmol g^{-1} h^{-1}**	**This work**

(*) Represents reaction performed in continuous flow with AI.

References

1. X. Xue, Y. Weng, S. Yang, S. Meng, Z. Zhang, G. Yi and Y. Zhang, *Environ. Sci. Pollut. Res. Int.*, 2021, **28**, 15883-15889.
2. I. Mondal and U. Pal, *Phys. Chem. Chem. Phys.*, 2016, **18**, 4780-4788.
3. H. Lee, J.-H. Lee, Y. Lee, E.-B. Cho and Y. J. Jang, *Appl. Surf. Sci.*, 2023, **620**, 156812.
4. B.-H. Lee, S. Park, M. Kim, A. K. Sinha, S. C. Lee, E. Jung, W. J. Chang, K.-S. Lee, J. H. Kim, S.-P. Cho, H. Kim, K. T. Nam and T. Hyeon, *Nat. Mater.*, 2019, **18**, 620-626.
5. M. Wang, M. Liu, J. Lu and F. Wang, *Nat. Commun.*, 2020, **11**, 1083.
6. A. Tiwari, A. Goutam, S. Sk, P. Vijayanand, B. M. Abraham and U. Pal, *Int. J. Hydrogen Energy*, 2023, **48**, 29178-29188.
7. S.-Y. Xu, W. Shi, J.-R. Huang, S. Yao, C. Wang, T.-B. Lu and Z.-M. Zhang, *Angew. Chem. Int. Ed.*, 2024, **63**, e202406223.
8. C. Pan, H. Shen, G. Liu, X. Zhang, X. Liu, H. Liu, P. Xu, W. Chen, Y. Tian, H. Deng, H. Sun, J. Wang, Z. Luo, L. Zhang and Y. Guo, *ACS Appl. Nano Mater.*, 2022, **5**, 10980-10990.
9. Y.-S. Ouyang, S.-T. Zheng, G.-W. Guan and Q.-Y. Yang, *ACS Appl. Energy Mater.*, 2022, **5**, 14455-14465.
10. E. Liu, L. Kang, F. Wu, T. Sun, X. Hu, Y. Yang, H. Liu and J. Fan, *Plasmonics*, 2014, **9**, 61-70.
11. W. Wang, D. Xu, B. Cheng, J. Yu and C. Jiang, *J. Mater. Chem. A*, 2017, **5**, 5020-5029.
12. Y. Wang, R. Godin, J. R. Durrant and J. Tang, *Angew. Chem. Int. Ed.*, 2021, **60**, 20811-20816.
13. K. Wang, M. Cheng, F. Xia, N. Cao, F. Zhang, W. Ni, X. Yue, K. Yan, Y. He, Y. Shi, W. Dai and P. Xie, *Small*, 2023, **19**, 2207581.
14. Z. Zhang, R. Chen, L. Wang, X. Chen, J. Ding, J. Zhang, H. Wan and G. Guan, *Appl. Surf. Sci.*, 2023, **609**, 155297.
15. P. Athikaphan, S. Neramittagapong, P. Assawasaengrat and A. Neramittagapong, *Energy Reports*, 2020, **6**, 1162-1166.
16. F. Iqbal, A. Mumtaz, S. Shahabuddin, M. I. Abd Mutalib, M. S. Shaharun, T. D. Nguyen, M. R. Khan and B. Abdullah, *J Chem Technol Biotechnol*, 2020, **95**, 2208-2221.
17. M. Abou Asi, C. He, M. Su, D. Xia, L. Lin, H. Deng, Y. Xiong, R. Qiu and X.-z. Li, *Catal. Today*, 2011, **175**, 256-263.
18. P. Kumar, C. Joshi, N. Labhsetwar, R. Boukherroub and S. L. Jain, *Nanoscale*, 2015, **7**, 15258-15267.
19. C. Tang, W. Hou, E. Liu, X. Hu and J. Fan, *J. Lumin.*, 2014, **154**, 305-309.
20. Y. A. Wu, I. McNulty, C. Liu, K. C. Lau, Q. Liu, A. P. Paulikas, C.-J. Sun, Z. Cai, J. R. Guest, Y. Ren, V. Stamenkovic, L. A. Curtiss, Y. Liu and T. Rajh, *Nat. Energy*, 2019, **4**, 957-968.